

Lubricant Thickness Effect on Tribological Performance of ZDOL Lubricated Disks with Hydrogenated Overcoats

Chao-Yuan Chen, Walton Fong, and David B. Bogy

Computer Mechanics Laboratory
Department of Mechanical Engineering
University of California at Berkeley, CA 94720

C. Singh Bhatia

SSD/IBM, 5600 Cottle Road, San Jose, CA 95193

Abstract

Tribo-chemical studies of the lubricant thickness effect on the tribology of the head/disk interface (HDI) were conducted using hydrogenated (CH_x) carbon disk samples coated with perfluoropolyether ZDOL lubricant. The studies involved drag tests with uncoated and carbon-coated Al_2O_3 -TiC sliders and thermal desorption experiments in an ultra-high vacuum (UHV) tribochamber. The studies showed that the lubricant interaction with the carbon overcoat varies as a function of lubricant thickness. Wear durability improves considerably for thicknesses than a monolayer. However, in the sub-monolayer thickness regime, the adhesion of the lubricant to the carbon overcoat is much stronger, as indicated by the fact that a much higher temperature is required to desorb the lubricant. When the lubricant thickness is around or above a monolayer, cohesion among the lubricant molecules plays a greater role and a much lower temperature is needed for lubricant desorption.

Keywords: Tribochemistry; Hydrogenated carbon overcoat; ZDOL decomposition; Friction and wear; Thermal desorption

I. INTRODUCTION

Perfluoropolyethers (PFPE) are employed as lubricants in magnetic recording disk drives to reduce friction and wear. The PFPE lubricant and the hard carbon overcoat on the disks provide the necessary protection of the underlying magnetic film against wear due to sliding at the head-disk interface. Their decomposition mechanisms associated with contact sliding have been extensively studied. Many experiments demonstrate that PFPEs, subjected to electron irradiation, are easily decomposed into smaller fragments [1]. Vurens et al. [2] used low energy electrons to bombard PFPEs and observed that their electron decomposition occurs at an energy below their ionization potential (about 14 eV). It is reported that the decomposition rates of PFPEs are higher in the presence of Lewis acid forming materials, such as Fe_2O_3 [3], Al_2O_3 and AlCl_3 [4]. Our earlier studies of the decomposition of ZDOL lubricant on nitrogenated carbon overcoats (CN_x) [5] indicate that the decomposition rate is significantly affected by the slider materials. The use of uncoated Al_2O_3 -TiC sliders leads to the rapid decomposition of ZDOL due to catalytic reactions, while carbon coated sliders produce less intense decomposition due primarily to frictional actions [6]. The thermal stability of PFPE has also been studied extensively. Lin et al. [7] used temperature-programmed reaction/desorption (TRP/D) and electron simulated desorption (ESD) to study the roles of temperature and turboelectric charge in the decomposition of the Fomblin-ZDOL lubricant. They showed that the threshold temperature for its dissociation is 500-550K, in accordance with the known thermal stability of free ZDOL. Vurens [8] also showed that molecules having a $\text{CF}_2\text{-CF}_3$ endgroup (Demnum S65) display enhanced thermal stability compared to molecules with the $\text{CF}_2\text{-CF}_2\text{-CH}_2\text{-CH}_2\text{O-phenyl}$ endgroup (Demnum SP). Gellman [9] showed that the heat of adsorption of hydrocarbon ether

was greater than that of the corresponding fluorocarbon ether, suggesting that the ethers are bonded to the films through the donation of electron pairs on the oxygen atom. Gellman also proposed a model in which the electropositive nature of the hydrogen in the a-CH films weakens the extent of electron donation from the ether lone pairs and, hence, weakens the bonding of the ethers to the a-CH films. Furthermore, Perry [10] used temperature-programmed desorption and scanning force microscopy to probe the interaction of ZDOL with both hydrogenated carbon overcoats and nitrogenated carbon overcoats. The data showed that the nitride surfaces are more reactive toward the ZDOL lubricant and, as a result, the thin lubricant film is more tightly bound to the overcoats. In our previous report [11], the friction and catalytic decomposition mechanisms as well as the thermal behavior of ZDOL are described, and data demonstrating the chemical reactions of the lubricant and carbon overcoat are also presented.

The thickness of the PFPE lubricant layer must be chosen carefully to provide maximum wear protection and acceptable life performance. If the lubricant film is too thick, excessive stiction is observed upon start up of the drive. On the other hand, if the lubricant film is too thin, insufficient protection of the head-disk interface is provided, and tribological failure can occur in the early operating period. The trend in the industry in recent years has been to decrease the amount of lubricant used. Lubricant thicknesses of a single layer or less (sub-monolayer) are becoming quite common in disk drives. Therefore, the interactions between the lubricant and the carbon surface may be more important to the tribological performance of the disk drive than the bulk properties of PFPE lubricants.

Tyndall et al. [12] used surface energy measurements to extract information about the PFPE lubricant-carbon interfacial interactions. They measured the dispersive surface energy to determine the lubricant coverage of the carbon surface and yield information on the relative orientation of the lubricant backbone with respect to the carbon surface. They found that the surface energy of PFPE lubricated disks decreases with increasing lubricant thickness. Waltman et al. [13] showed that the surface energy of a bonded lubricant is substantially lower than that of a mobile lubricant, reflecting the increased interaction strength that occurs as a result of bonding. In the case of bonded ZDOL, the nonpolar nature of the lubricant/carbon combination indicates that much stronger interactions occur between the hydroxyl end-groups of ZDOL and the carbon surface. Also, Karis et al. [14] showed that the polar component of the surface energy for ZDOL exhibits oscillations as a function of lubricant thickness. As the amount of lubricant applied to the surface increases, the surface energy decreases since the fraction of the high-energy carbon surface covered by the low surface energy PFPE increases. Neutralization of the surface active sites by the addition of hydroxyl terminated ZDOL results in a decrease in the measured surface energy with increasing ZDOL thickness. A local minimum in the polar surface energy results at the point where the number of lubricant end-groups matches the number of active oxide sites on the carbon surface. Matching of the ZDOL end-group density with active site density on the carbon surface results in the complete coverage of the carbon surface by ZDOL lubricant.

In this report, we study the ZDOL thickness effect on hydrogenated carbon films (CH_x) using an ultra-high vacuum (UHV) tribochamber equipped with a mass spectrometer. The studies consist of drag tests and thermal desorption experiments in the UHV tribochamber. Two decomposition processes of ZDOL under sliding friction conditions are studied, one is with a

carbon film coated slider/CHx coated disk system, and another is with an uncoated Al₂O₃-TiC slider/CHx coated disk system. We illustrate the lubricant thickness effect on the tribological performance as well as the strength of the bonding between the lubricant and the carbon surface.

II. EXPERIMENTAL PROCEDURE AND SET-UP

The UHV tribochamber consists of a disk spindle, a slider actuator, a substrate heater, and a high-resolution quadrupole mass spectrometer (QMS) in a vacuum chamber with base pressure $< 2 \times 10^{-8}$ Torr, which was described in details in a previous paper [15]. The QMS provides in-situ detection of the gaseous products generated during drag tests and thermal desorption studies. The QMS can monitor simultaneously 15 different atomic mass units (AMUs) ranging from 1 to 500 along with friction or temperature data from strain gauge transducers or a thermocouple, respectively. It is noted that all AMUs from 1 to 192 of ZDOL decomposition products generated at the Al₂O₃/TiC slider/CHx disk interface were previously investigated under the same test conditions and only the most pertinent AMUs were monitored in this study.

Drag tests in the tribochamber were conducted as follows. Initially, the tribochamber was baked out at 150°F at high vacuum for 24 hours. The chamber was then backfilled with Argon gas as the disk and slider samples were mounted inside. Next, the chamber was pumped down to a base pressure of 2×10^{-8} Torr and the channels of the QMS were assigned to selected AMUs. Background intensities were recorded before the drag tests were initiated with the following parameters: 0.2 m/s drag speed, a load of 30 mN, and a sliding time of 20 minutes. The sliders

were 30% (1.2mm by 1mm) negative-pressure $\text{Al}_2\text{O}_3/\text{TiC}$ sliders with and without amorphous carbon films on the air bearing surfaces. The disks were commercial 95mm smooth thin film disks with a 75\AA amorphous hydrogenated carbon overcoat (CHx). The hydrogen content in the CHx film was 5 atomic percent. The disks were lubricated with ZDOL by a dipping process. The resulting thickness of ZDOL on the disks in this study were 4.5\AA , 6.2\AA , 9\AA , 12.5\AA , and 15.4\AA .

In preparation for the thermal desorption tests in the tribochamber the heater was baked at 600°F at high vacuum for 4 hours to bake out the residual lubricants left on the heater after each thermal desorption test. A CHx/ZDOL disk was cut into 2cm squares. The lubricated samples were mounted on the heater and the temperature was measured by a thermocouple in contact with the heater near the heated sample. As with the drag tests, the chamber was pumped down to 10^{-8} Torr and the channels of the QMS were assigned to selected AMUs. A typical experiment consisted of heating a sample at a rate of $0.3^\circ\text{F}/\text{sec}$ starting at room temperature and stopping before 500°F . A mass spectrum was collected on a computer every two seconds during the heating. Afterwards, the spectra were analyzed in order to obtain the thermal desorption profile for each mass as a function of sample temperature.

III. Results and discussion

A. Results from the UHV drag tests

In this section, we present the results from the UHV drag tests. Figures 1 through 5 part (a) show the friction coefficient curves for the ZDOL lubricated CHx disks against an uncoated and

a carbon coated $\text{Al}_2\text{O}_3/\text{TiC}$ pico slider. Before starting the friction tests, the background intensities were recorded for 80 seconds by the mass spectrometer. Figures 1 through 5 part (b) show the integrated mass spectra of ZDOL fragments produced from the head-disk interface. The four primary peaks are for mass fragments CFO (47), CF_2O (66), CF_3 (69), and C_2F_5 (119). In our previous studies of CHx carbon overcoats paired with carbon-coated sliders [11], the primary mechanism of ZDOL was due to frictional effects, and it was characterized by the generation of CFO (47), and CF_2O (66). The absence of a carbon-coating led to a more complex catalytic decomposition mechanism of ZDOL, and it was characterized by the generation of CF_3 (69) and C_2F_5 (119).

Figure 1(a) shows the friction coefficient curves for the 4.5\AA ZDOL lubricated disk. For the 100\AA DLC coated $\text{Al}_2\text{O}_3/\text{TiC}$ slider, the friction coefficient started at 0.3 and became very unstable immediately. A wear track was observed on the disk after just 10 drag cycles. The friction variation, as shown in figure 1(a), is most likely due to three body contact resulting from small wear particles that were generated at the head-disk interface. For the uncoated $\text{Al}_2\text{O}_3/\text{TiC}$ slider, the friction coefficient increased to a peak value of 1.3 immediately and dropped to 0.3 after reaching its peak value. A wear track was observed on the disk just after the friction coefficient dropped. The above results indicate that ZDOL of 4.5\AA thickness has little lubricating action against both the uncoated and the DLC coated $\text{Al}_2\text{O}_3/\text{TiC}$ sliders. Figure 1(b) shows the integrated mass spectra of four major ZDOL decomposed fragments produced from the head-disk interface. This mass spectrum for the 100\AA DLC coated $\text{Al}_2\text{O}_3/\text{TiC}$ slider is similar to that of ZDOL vapor as reported by Kasai et al. [4], where the primary decomposition peaks are masses 47 (CFO) and 66 (CF_2O) due to frictional heat [11]. Because no contact with

Lewis acid is possible in this case, the ZDOL decomposition is attributed to friction/thermal actions only, and therefore it should be directly related to the molecular bond energies. The relevant bond dissociation energy [16] is used to judge the bond strength and possible decomposition trends. Because the weakest bonds in ZDOL are C-O-C and C-C, the ZDOL molecule is expected to cleave preferentially at these locations. A radical mechanism proposed by Sianesi et al. [17] postulates that PFPEs dissociate by breaking the weaker C-C bonds followed by β scission to form perfluorinated aldehyde and alkene. Therefore, masses 47 (CFO) and 66 (CF₂O) are the primary fragments due to frictional heat action. For the uncoated Al₂O₃/TiC slider, the mass intensities of the four major ZDOL fragments are almost one order higher than those in the DLC coated slider case. The decomposition mechanisms of ZDOL in the case of the uncoated Al₂O₃/TiC slider are much more complicated than those with the DLC coated slider. For the uncoated slider, catalytic reactions control the ZDOL decomposition and the catalytic reactions lead to the generation of masses 69 (CF₃) and 119 (C₂F₅). In figure 1(b), mass 69 (CF₃) is the highest peak in the uncoated slider case as shown in figure 1(b).

Figure 2(a) shows the friction coefficient curves for the **6.2Å ZDOL** lubricated disk. For the 100Å DLC coated Al₂O₃/TiC slider, the friction coefficient started at 0.3 and became very unstable immediately. A wear track was observed on the disk after 16 drag cycles. For the uncoated Al₂O₃/TiC slider, the friction coefficient increased to a peak value of 0.5 immediately and dropped to 0.3 after reaching its peak value. A wear track was observed on the disk just after the friction coefficient dropped. These results are very similar to those of the 4.5Å ZDOL disk. The above results indicate that a disk with 6.2Å ZDOL has little lubricating action against both the uncoated and the DLC coated Al₂O₃/TiC sliders. Moreover, there is no added benefit in

using 6.2Å of ZDOL versus 4.5Å of ZDOL. Figure 2(b) shows the integrated mass spectra of four major ZDOL decomposition fragments produced from the head-disk interface. For the 100Å DLC coated Al₂O₃/TiC slider, the primary decomposed peaks are masses 47 (CFO) and 66 (CF₂O). For the uncoated Al₂O₃/TiC slider, mass 69 (CF₃) is the highest peak due to catalytic reactions. When the ZDOL thickness increases from 4.5Å to 6.2Å, the degradation intensities of the four major decomposition fragments increase. These results along with those described below, indicate that the degradation of ZDOL lubricant increases with increased thickness.

Figure 3(a) shows the friction coefficient curves for the 9Å ZDOL lubricated disk. For the 100Å DLC coated Al₂O₃/TiC slider, the friction coefficient started at 0.3 and increased steadily to 0.7 within 195 drag cycles before wear occurred. For the uncoated Al₂O₃/TiC slider, the friction coefficient increased to a peak value of 1.6 immediately and dropped to 0.4 after reaching its peak value. A wear track was observed on the disk just after the friction coefficient dropped. These results are different from those for the 4.5Å ZDOL or 6.2Å ZDOL disks. These results indicate that 9Å of ZDOL has good lubricating action against the DLC coated slider, but it provides little protection against the uncoated slider. Furthermore, we clearly see some benefit of using 9Å of ZDOL versus 4.5Å or 6.2Å of ZDOL in the DLC coated slider case. Figure 3(b) shows the integrated mass spectra of four major ZDOL decomposition fragments produced from the head-disk interface. For the 100Å DLC coated Al₂O₃/TiC sliders, the primary decomposition peaks are masses 47 (CFO) and 66 (CF₂O). When the ZDOL thickness increases from 6.2Å to 9Å, the degradation intensities of the four major decomposition fragments remain the same for the DLC coated slider case. For the uncoated slider, the intensities of masses 69 and 119 increased almost one order of magnitude when the ZDOL thickness increased from 6.2Å to 9Å,

while the intensities of mass 47 and mass 66 remained the same. These results indicate that strong catalytic reactions occur with the uncoated slider when the ZDOL thickness is 9Å.

Figure 4(a) shows the friction coefficient curves for the **12.5Å ZDOL** lubricated disk. For the 100Å DLC coated Al₂O₃/TiC slider, the friction coefficient started at 0.4 and increased steadily to 0.8 after 700 drag cycles, where the drag test was stopped. No wear track was observed on the disk surface. For the uncoated Al₂O₃/TiC slider, the friction coefficient increased to a peak value of 2.4 immediately and dropped to 0.8 after reaching its peak value. A wear track was observed on the disk after 65 drag cycles. The above results indicate that 12.5Å of ZDOL has very good lubricating action against the DLC coated slider, but little protection against the uncoated slider. Nonetheless, 12.5Å of ZDOL provides some greater benefit than 9Å of ZDOL in drag tests with both coated and uncoated sliders. Enhanced wear durability is achieved by using thicker ZDOL lubricant against DLC coated sliders. More discussion will be presented later. Figure 4(b) shows the integrated mass spectra of four major ZDOL decomposed fragments produced from the head-disk interface. For the 100Å DLC coated Al₂O₃/TiC slider, the primary decomposition peaks are mass 47 (CFO) and mass 66 (CF₂O). For the uncoated Al₂O₃/TiC slider, mass 69 (CF₃) is the highest peak due to the catalytic reactions. These results are consistent with those presented earlier. However, the intensities of masses 69 and 119 are significantly higher than those of masses 47 and 66 for the uncoated slider case. Once again, increasing the ZDOL thickness (from 9Å to 12.5Å), increases the degradation intensities of the four major decomposition fragments - 40% for the DLC coated slider case and 500% for the uncoated slider case. These results indicate that strong catalytic reactions occur with the

uncoated slider when the lubricant thickness is 12.5Å. Further explanation will be given later based on the thermal desorption data.

Figure 5(a) shows the friction coefficient curves for the **15.4Å ZDOL** lubricated disk. For the 100Å DLC coated Al₂O₃/TiC slider, the friction coefficient started at 0.5 and increased steadily to 1.1 after 700 drag cycles, where the drag test was stopped. No wear track was observed on the disk surface. For the uncoated Al₂O₃/TiC slider, the friction coefficient increased to a peak value of 2.4 immediately and dropped to 0.9 after reaching its peak value. A wear track was observed on the disk after 60 drag cycles. Once again, good wear durability was observed with the DLC coated slider, while the uncoated slider case failed immediately. There is no apparent benefit from using 15.4Å of ZDOL versus 12.5Å of ZDOL with uncoated sliders. Figure 5(b) shows the integrated mass spectra of four major ZDOL decomposed fragments produced from the head-disk interface. For the 100Å DLC coated Al₂O₃/TiC sliders, the primary decomposition peaks are mass 47 (CFO) and mass 66 (CF₂O). For the uncoated Al₂O₃/TiC sliders, mass 69 (CF₃) is the highest peak due to the catalytic reactions. These results are similar to those shown earlier. There is no significant increase in the intensities of the four major ZDOL decomposition fragments when the thickness increases from 12.5Å to 15.4Å.

Figure 6 shows the degradation intensities of (a) mass 47 (CFO) and (b) mass 66 (CF₂O) during UHV drag tests on CHx disks with different ZDOL thicknesses. The degradation intensities of the frictional fragments 47 (CFO) and 66 (CF₂O) increased one order of magnitude with uncoated sliders when the thickness of ZDOL exceeded 12Å. However, no such increase was noted with disks tested against DLC coated sliders. Figure 7 shows similar result for the

catalytic fragments 69 (CF₃) and 119 (C₂F₅). Figure 8 shows the wear durability of these CHx disks as a function of ZDOL thickness. With DLC coated sliders, the wear durability was significantly improved when the lubricant thickness exceeded 12Å. These results explain the better wear durability of using thicker ZDOL - a thicker layer of ZDOL provides more lubricant to be decomposed so the carbon overcoat surface is protected for a longer duration against sliding. However, there was no benefit in using thicker lubricant for the uncoated slider cases. Strong catalytic reactions occurred with the uncoated slider when the ZDOL thickness exceeded 12Å. These catalytic reactions counteract the benefits of using thicker ZDOL, so 9Å of ZDOL performs as poorly as 4.5Å or 6.2Å of ZDOL with an uncoated slider..

With DLC coated sliders, the wear durability of disks lubricated with ZDOL significantly improves when the lubricant thickness exceeds 12Å. This enhanced performance with thicker ZDOL may be due to two mechanisms: (1) full coverage of the carbon surface with ZDOL, and (2) a thicker layer of mobile ZDOL to reflow into the wear track. Using surface energy (dispersive & polar) of ZDOL on carbon-coated disks, Karis et al. [14] showed that complete coverage of the disk surface occurs at 10Å for ZDOL 1600 and 15Å for ZDOL 3100. Tyndall et al. [12] also measured the surface energy for ZDOL on carbon-coated disks and found that complete coverage of the carbon surface occurs at $14 \pm 2\text{Å}$ for ZDOL 2000. These results support the first mechanism we cited for improvement in wear durability – at 12Å, the surface is completely covered.

The second mechanism for improved wear durability may be attributed to the refill of the mobile ZDOL layer in the track area. . We used FTIR to measure the lubricant thickness of these

disks before the UHV drag tests. These FTIR thickness measurements were confirmed by ellipsometry, and X-ray reflectivity. After the thicknesses were measured, the disks were washed in perfluorohexane and 2,3-dihydro-perfluoropentane to remove any soluble lubricant [18], and then the thickness was remeasured. The lubricant that is retained on these disks is defined as the amount “bonded”, while the portion removed by the solvent wash process is defined as the “mobile” portion. The results are summarized in the following table:

| Disks | Bonded Thickness (Å) | Mobile Thickness (Å) |
|-------------------|-----------------------------|-----------------------------|
| 4.5Å ZDOL | 3.3 | 1.2 |
| 6.2Å ZDOL | 4.7 | 1.5 |
| 9Å ZDOL | 5.7 | 3.3 |
| 12.5Å ZDOL | 7.9 | 4.6 |
| 15.4Å ZDOL | 10.4 | 5 |

Figure 9 is a plot of the wear durability vs. the mobile ZDOL thickness during UHV drag tests. For the disks tested with 70Å DLC coated sliders, the wear durability improves considerably with thicker mobile ZDOL. These results reflect the importance of the mobile ZDOL layer in providing good wear durability. We believe the role of the mobile layer is to replenish the lube displaced during dragging. As lube thickness increases, the replenishment rate also increases as suggested by O,Connor et al.[19] and Ma et al. [20,21,22] in their studies of the spreading behavior of PFPE on silica surfaces. In their paper, Ma suggests that the functional end-groups of ZDOL significantly retard the diffusion process, owing probably to their stronger interactions with the carbon surface. In the context of our study, as the lubricant thickness increases, the end-group effect on the diffusion process decreases, and the diffusion coefficient increases. As a result, faster replenishment of the lubricant occurs on disks with thicker ZDOL on the protective carbon surface, enhancing the wear durability at the interface.

B. Results from UHV thermal desorption tests

In this section, we present and discuss the results from UHV thermal desorption experiments. Figure 10 shows the thermal desorption history profiles for masses 47 (CFO) and 66 (CF₂O) of CHx disks with different ZDOL thickness ranging from 4.5Å to 15.4Å at a heating rate of 0.3F/sec. These two fragments are characteristic of friction/mechanical shear actions and electron bombardment [11] in drag tests. Figure 11 shows the thermal desorption history profiles for masses 69 (CF₃) and 119 (C₂F₅) of CHx disks with different ZDOL thickness ranging from 4.5Å to 15.4Å. These two fragments are used to monitor the catalytic decomposition. Two thermal desorption peaks were found during these experiments: one is between 100°F and 200°F, and the other is between 250°F and 450°F. We used FTIR to measure the lubricant thickness of the samples before and after the thermal desorption experiments. We will describe the procedure for the 9Å ZDOL disk – it is similar for the others. Three samples (labeled A, B, and C) were cut from the same 9Å ZDOL disk and measured. Sample A did not go through the thermal desorption test; sample B was heated just past the first thermal desorption peak (100°F to 200°F); sample C was tested up to the temperature of 400°F (after going through the first and second thermal desorption peaks). The measurements are listed below:

| | Sample A | Sample B | Sample C |
|------------------|----------|----------|----------|
| total thickness | 8.5Å | 6.2Å | 0.7Å |
| bonded thickness | 5.2Å | 5.8Å | * |
| mobile thickness | 2.3Å | 0.4Å | * |

* could not measure

From the data, we conclude that most of the mobile lubricant is desorbed during the first thermal desorption period, and the bonded lubricant increased 0.6Å due to the annealing effect at

temperatures above 150°F. These results are similar to those found by Waltman et al. [17]. They found that the initially applied mobile ZDOL is depleted via evaporative loss as well as bonding of the lubricant to active sites on the carbon surface at the elevated temperatures between 60°C to 150°C, which is the operating temperature of the disk drives. The relative branching into the evaporation and bonding channels is molecular weight dependent, with increasing molecular weight favoring bonding. The activation energy for ZDOL evaporation is highly dependent on molecular weight, decreasing rapidly with decreasing molecular weight. Therefore, the lower molecular weight components present in ZDOL 2000 will preferentially evaporate from the disk surface. In our current case of ZDOL 2000 (low molecular weight), evaporation is the dominant channel responsible for the depletion of mobile ZDOL 2000, and only 0.6Å mobile ZDOL became bonded on the carbon surface. Samples C shows that most of the ZDOL lubricant is desorbed by 400°F. Thus, we can conclude that only the mobile ZDOL layer is desorbed during the first thermal desorption period and the residual bonded ZDOL layer is desorbed during the second thermal desorption period. This indicates that the desorption energy of bonded ZDOL lubricant is higher than that of mobile ZDOL lubricant. Waltman et al. [13] also showed similar results in that the surface energy of the bonded lubricant is substantially lower than the mobile lubricant, reflecting the increased interaction strength that occurs as a result of bonding.

Figures 10 and 11 illustrate that CFO (47) and CF₂O (66) are the primary thermal desorption fragments from the first peak, which corresponds to desorption of the mobile ZDOL layer. These results are consistent with those of Lin and Kasai [7,24]. During the second thermal desorption peak (between 250°F and 450°F), the bonded ZDOL layer was desorbed and all four primary fragments were observed. When the lubricant thickness is below 9Å (4.5Å and 6.2Å in

our study), the generation of fragments associated with friction heat/electron bombardment (CFO and CF₂O) is much higher than that of the catalytic related fragments (CF₃ and C₂F₅). However, when the lubricant thickness reaches 9Å and higher (9Å, 12.5Å, and 15.4Å in our study), the intensity of the catalytic related fragment (CF₃) equals that of the friction heat/electron bombardment associated fragments (CFO and CF₂O). The generation of fragment CF₃ may be a consequence of the desorption of bonded lubricant from the CH_x surface [11].

Moreover, the ZDOL desorbed peak temperatures shifted to lower temperatures with increasing lubricant thickness. Figure 12 shows the thermal desorption peak temperatures of ZDOL for CH_x disks with ZDOL thickness ranging from 4.5Å to 15.4Å. The temperature at the first peak, which is attributed to the desorption of the mobile ZDOL layer, remains almost constant as a function of ZDOL thickness. This result indicates that the desorption energy of the mobile ZDOL layer is independent of the lubricant thickness. However, the temperature at the second peak, corresponding to the desorption of bonded ZDOL, shifts to a lower temperature with increasing ZDOL thickness as shown in figure 12. This result indicates that the desorption energy of bonded lubricant decreases with increasing lubricant thickness. One possible explanation is that the surface of the amorphous carbon is populated with sites of different interaction strengths, where stronger bond sites are associated with higher binding energy [9]. When ZDOL molecules adsorb on the surface, they first occupy the stronger sites (sites with higher desorption energy). As more ZDOL molecules (thicker lubricant) are adsorbed, weaker sites (sites of lower desorption energy) are occupied. Thus, at thinner ZDOL the second peak temperature is higher, and it is lower for thicker ZDOL. Earlier UHV drag tests show that strong catalytic reaction occurs for the uncoated slider case when the lubricant is thicker. With thicker

ZDOL, the thermal desorption energy of bonded lubricant decreases, so the decomposition of ZDOL is easier as well as the catalytic reaction.

Figure 13 shows the integrated thermal desorption intensity of CFO (47) versus (a) mobile ZDOL thickness during the first desorption peak, and (b) bonded ZDOL thickness during the second desorption peak. The integrated intensity of the fragment CFO during the first desorption peak increases as thicker mobile ZDOL layer is desorbed. However, the intensity - thickness curve does not have a linear relationship as shown in figure 13 (a). In our earlier result, we found that, at the first desorption peak, evaporation is the dominant channel for the depletion of mobile ZDOL 2000, but a small portion of mobile ZDOL 2000 is bonded on the carbon surface. Thus, the integrated desorption intensity of CFO is not exactly proportional to the original mobile ZDOL thickness at the first desorption peak. The desorption intensity of this fragment is, however, almost proportional to the bonded ZDOL thickness at the second desorption peak, as shown in figure 13 (b). The small fraction of bonded ZDOL originating from the mobile ZDOL will not affect the linearity of the intensity thickness curve shown in figure 13 (b). These results further support the assertion that the bonded ZDOL layer was desorbed during the second peak.

IV. Conclusion

The experiments presented here illustrate the complex chemical relationships that occur at the head/disk interface during drag tests. The UHV tribochamber was used to monitor in situ the gaseous wear products generated at the HDI during dragging. UHV drag tests show that the lubricant interaction with the carbon overcoat varies as a function of lubricant thickness. Wear durability of ZDOL against DLC coated sliders improves considerably when the carbon overcoat surface is fully covered by one layer of ZDOL. This enhanced performance with thicker ZDOL can be due to two mechanisms: (1) full coverage of the carbon surface with ZDOL, and (2) a thicker layer of mobile ZDOL to reflow into the wear track. However, there was no benefit in using thicker lubricant for the uncoated slider cases. Strong catalytic reactions occurred with the uncoated slider when the ZDOL thickness exceeded 12Å. These catalytic reactions counteract the benefits of using thicker ZDOL.

Based on the thermal desorption experiments, only mobile ZDOL lubricant was desorbed at the first thermal desorption peak (between 100°F and 200°F), and the residual bounded ZDOL lubricant was desorbed at the second thermal desorption peak (between 250°F and 450°F). In the sub-monolayer regime, adhesion of lubricant to the carbon overcoat is much stronger because it requires a much higher temperature to desorb the lubricant molecule. When the lubricant thickness is around or above a monolayer, cohesion among the lubricant molecules plays a greater role and a much lower temperature is needed for lubricant desorption.

ACKNOWLEDGMENTS

This work was supported by the Computer Mechanics Laboratory at the University of California, Berkeley. The authors would like to thank Dr. R.J. Waltman of IBM, and Dr. M. Donovan of Read-Rite for preparation of the disks and sliders; Dr. Mark Karplus, Dr. Daryl Pocker of IBM for lubricant thickness measurement; and Dr. Tai Cheng of HMT and Dr. Waltman for their helpful discussions on lubricant decomposition.

REFERENCES

- [1] Pacansky J. and Waltman R. J., "Electron Beam Irradiation of Polyperfluoroethers: Experimental Analysis of Main-chain Degradation", *Chem.Mater.* 5, pp486-494, (1993).
- [2] Vurens G., Zehringer R. and Saperstein D., "The Decomposition Mechanisms of Perfluoropolyether Lubricants during Wear", *Surface Science Investigations in Tribology*, Chung Y.W., Homola A. M. and street B., Eds, Washington, D. C.: American Chemical Society, pp169-180, (1992)
- [3] M.J. Zehe and O. O. Faut, "Acid Attack of Perfluorinated Alkyl Ether Lubricant Molecules by Metal Oxide Surfaces", *Tribology Trans.*, 33, pp634-640, (1990)
- [4] P.H. Kasai, "Degradation of Perfluoropolyethers Catalyzed by Lewis Acids", *Adv. Info. Storage Syst.* 4., pp291-314, (1992)
- [5] Jianjun Wei, Walton Fong, D. B. Bogy and C. S. Bhatia, "The Decomposition Mechanisms of a Perfluoropolyether at the Head/Disk Interface of Hard Disk Drives", *Tribology Letters*, Vol. 5, pp203-209, (1998)
- [6] D. B. Bogy, X. H. Yun, and B. J. Knapp, "Enhancement of Head-Disk Interface Durability by Use of DLC Overcoats on the Slider's Rails", *IEEE Trans on Magnetics*, Vol. 30, No.5, pp369-373, (1994)
- [7] Jong-Liang Lin, C. Singh Bhatia, and John T. Yates, Jr., "Thermal and Electron-simulated Chemistry of Fomblin-ZDOL Lubricant on a Magnetic Disk", *J. Vac. Sci. Technol. A* 13(2), pp163-168, (1995)
- [8] G. H. Vurens and C. M. Mate, "The Thermal Stability of Perfluoropolyethers on Carbon Surfaces", *Applied Surface Science*, 59, pp281-287, (1992)

- [9] Laura Cornaglia and Andrew J. Gellman, "Fluoroether Bonding to Carbon Overcoats", *J. Vac. Sci. Technol. A* 15(5), pp2755-2765, (1997)
- [10] Scott S. Perry, Philip B. Merrill and Hyun I. Kim, "Comparative Studies of Perfluorinated Lubricants Adsorbed on Hydrogenated Amorphous Carbon and Amorphous Carbon Nitride", *Tribology Letters* 2, pp393-404, (1996)
- [11] C.Y. Chen, W. Fong, D. Bogy, and C. Bhatia, "The decomposition mechanisms and thermal stability of ZDOL lubricant on hydrogenated carbon overcoats", CML Technical Report No. 98-016, submitted to *Journal of Tribology*
- [12] G.W. Tyndall, P.B. Leezenberg, R.J. Waltman, and J. Castenada, "Interfacial interactions of Perfluoropolyether lubricants with magnetic recording media", *Tribology Letters* 4, pp103-108, (1998)
- [13] R.J. Waltman, D.J. Pocker, and G.W. Tyndall, "Studies on the interactions between ZDOL Perfluoropolyether lubricant and the carbon overcoat of rigid magnetic media", *Tribology Letters* 4, pp267-275 (1998)
- [14] T.E. Karis, G.W. Tyndall, and M.S. Jhon, "Spreading profiles of molecularly thin Perfluoropolyether films", submitted to *Tribology Trans.*, March 1998
- [15] X. H. Yun, D. B. Bogy, and C. S. Bhatia, "Tribochemical Study of Hydrogenated Carbon Coatings with Different Hydrogen Content Levels in Ultra High Vacuum", *J. Tribology*, 119, pp437-443, (1997)
- [16] A. Steritwieser, and C. H. Heathcock, "Introduction to Organic Chemistry", Macmillan Publishing Co., Inc., New York, (1976)
- [17] D. Sianesi, V. Zamboni, R. Fontanelli, and M. Binaghi, "Perfluoropolyethers: their physical properties and behavior at high and low temperatures", *Wear*, 18, pp85-100, (1971)

- [18] R.J. Waltman, and G.W. Tyndall, "The evaporation and bonding of ZDOL polyperfluorinated Ether lubricants on CH_x carbon overcoated rigid magnetic media", submitted to J. Phys. Chem.
- [19] T.M. O'Connor, M.S. Jhon, C.L. Bauer, B.G. Min, D.Y. Yoon, and T.E. Karis, "Surface diffusion and flow activation energies of perfluoropolyether", Tribology Letters 1, pp219-223, (1995)
- [20] X. Ma, J. GUI, L.Smoliar, K. Grannen, B. Marchon, M.S. Jhon, and C.L. Bauer, "Spreading of perfluoropolyether films on amorphous carbon surfaces", J. of Chemical Physics, vol. 110, no. 6, pp3129-3137, (1999)
- [21] X. Ma, J. Gui, K. Grannen, L.Smoliar B. Marchon, M.S. Jhon, and C.L. Bauer, "Spreading of PFPE lubricants on carbon surfaces: effect of hydrogen and nitrogen content", Tribology Letters, 6, pp9-14, (1999)
- [22] X. Ma, J. Gui, L.Smoliar, K. Grannen, B. Marchon, M.S. Jhon, and C.L. Bauer, "Complex terraced spreading of perfluoropolyether films on carbon surfaces", Physical Review E, vol. 59, no. 1, pp722-727, (1999)
- [23] C. Matano, J. of Physics, vol.8, pp109, (1932-1933)
- [24] P.H. Kasai, W.T. Tang and P. Wheeler, "Degradation of Perfluoropolyethers Catalyzed by Alumina Oxide", Appl. Surf. Sci. 51, pp201-211, (1991)

CAPTIONS

Figure 1: (a) friction coefficient of UHV drag test on 4.5Å ZDOL lubricated disk; (b) mass spectrum of four major ZDOL decomposed fragments.

Figure 2: (a) friction coefficient of UHV drag test on 6.2Å ZDOL lubricated disk; (b) mass spectrum of four major ZDOL decomposed fragments.

Figure 3: (a) friction coefficient of UHV drag test on 9Å ZDOL lubricated disk; (b) mass spectrum of four major ZDOL decomposed fragments.

Figure 4: (a) friction coefficient of UHV drag test on 12.5Å ZDOL lubricated disk; (b) mass spectrum of four major ZDOL decomposed fragments.

Figure 5: (a) friction coefficient of UHV drag test on 15.4Å ZDOL lubricated disk; (b) mass spectrum of four major ZDOL decomposed fragments.

Figure 6: integrated degradation intensity of ZDOL during UHV drag tests on CHx disks with different ZDOL thickness. Two major decomposed fragments under friction action: (a) mass 47 (CFO), and mass 66 (CF₂O).

Figure 7: integrated degradation intensity of ZDOL during UHV drag tests on CHx disks with different ZDOL thickness. Two major decomposed fragments under catalytic reactions: (a) mass 69 (CF₃), and mass 119 (C₂F₅).

Figure 8: wear durability of CHx disks with different ZDOL thickness during UHV drag tests against coated or uncoated Al₂O₃/TiC sliders.

Figure 9: wear durability of CHx disks with different mobile ZDOL thickness during UHV drag tests against coated or uncoated Al₂O₃/TiC sliders.

Figure 10: thermal desorption history profiles of mass 47 (CFO), and mass 66 (CF₂O) during the thermal desorption tests on CHx disks with different ZDOL thickness ranging from 4.5Å to 15.4Å.

Figure 11: thermal desorption history profiles of mass 69 (CF₃), and mass 119 (C₂F₅) during the thermal desorption tests on CHx disks with different ZDOL thickness ranging from 4.5Å to 15.4Å.

Figure 12: thermal desorbed peak temperatures of ZDOL for CHx disks with ZDOL thickness ranging from 4.5Å to 15.4Å.

Figure 13: integrated thermal desorption intensity of CFO (47) versus (a) mobile ZDOL thickness during the first desorption peak, and (b) bonded ZDOL thickness during the second desorption peak.

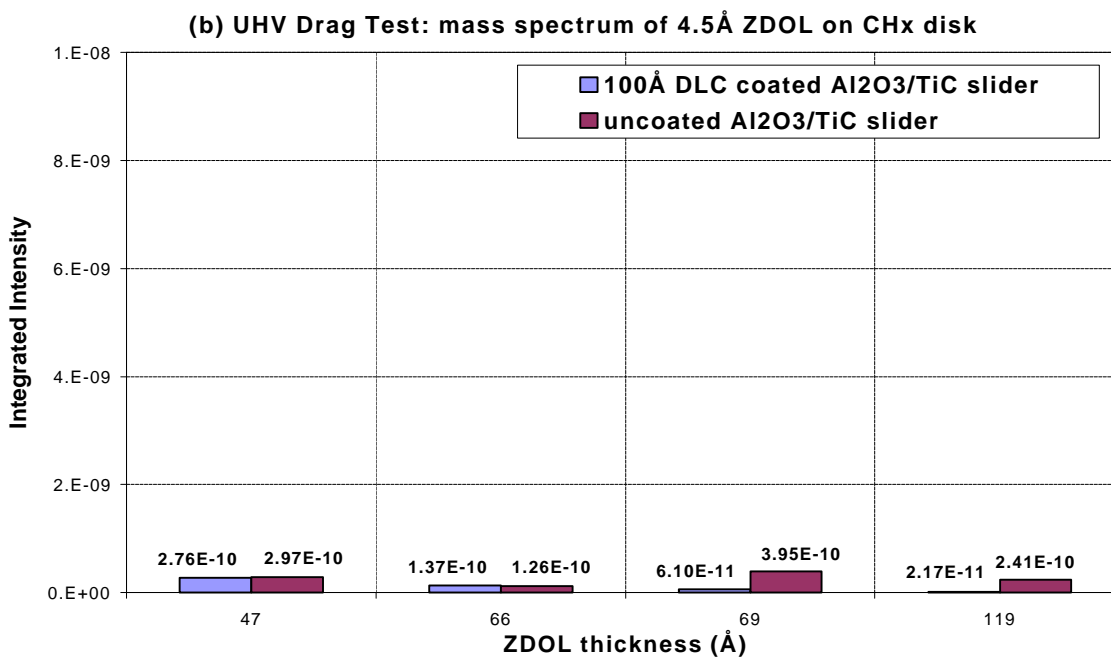
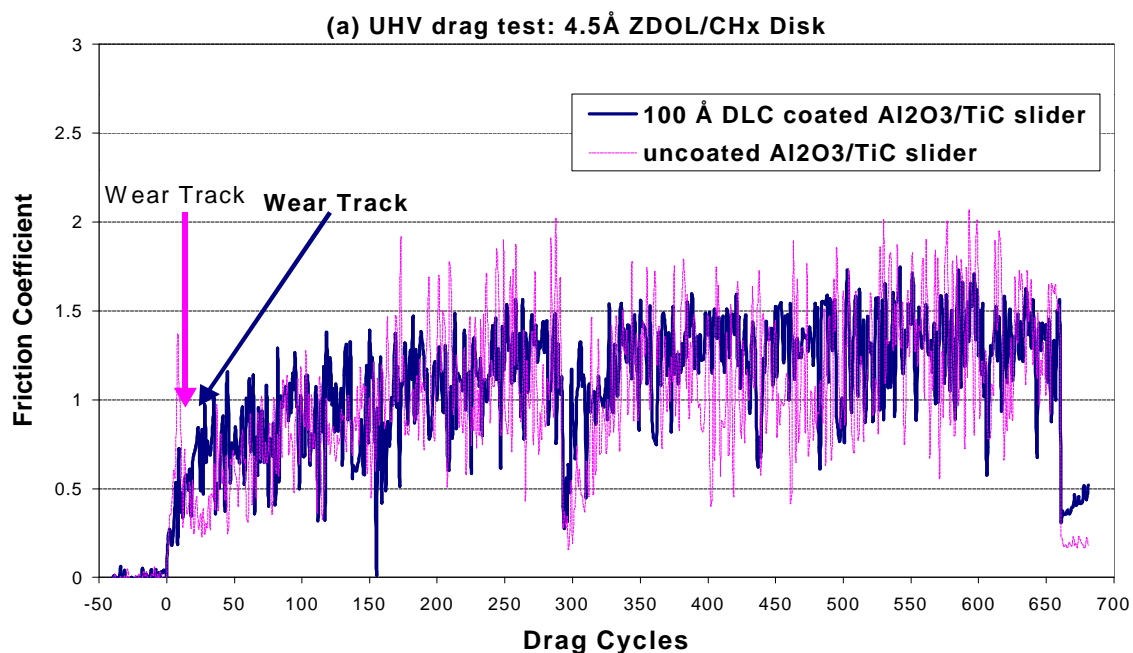


Figure 1: (a) friction coefficient of UHV drag test on 4.5Å ZDOL lubricated disk; (b) mass spectrum of four major ZDOL decomposed fragments.

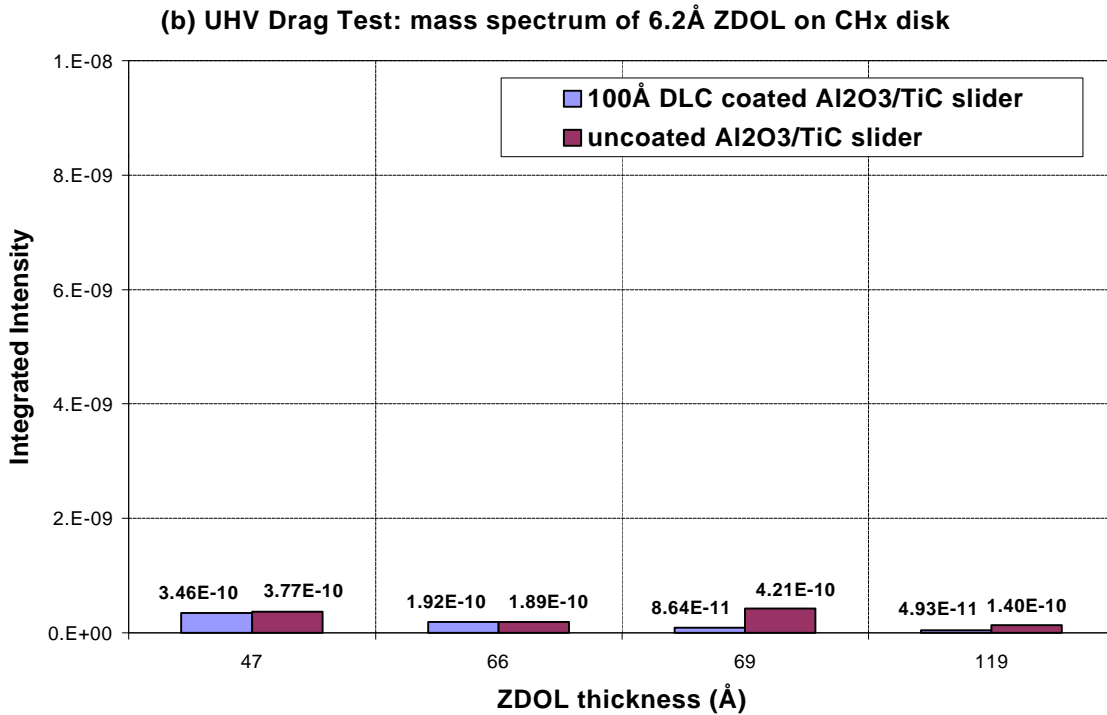
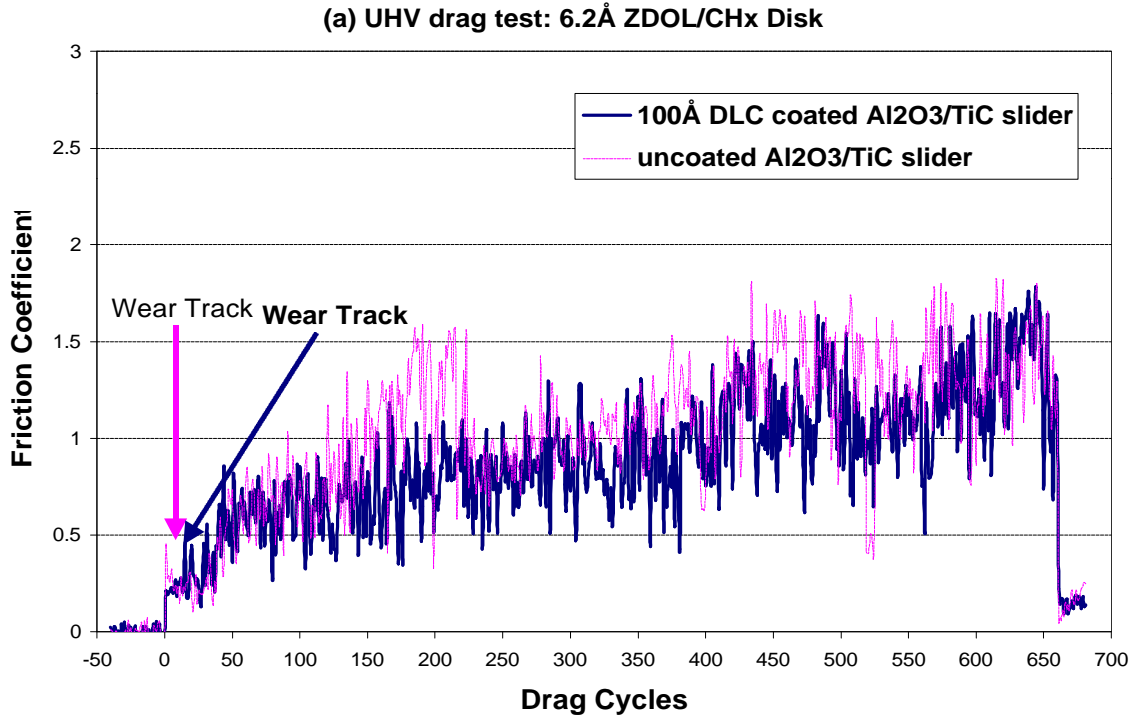


Figure 2: (a) friction coefficient of UHV drag test on 6.2Å ZDOL lubricated disk; (b) mass spectrum of four major ZDOL decomposition fragments.

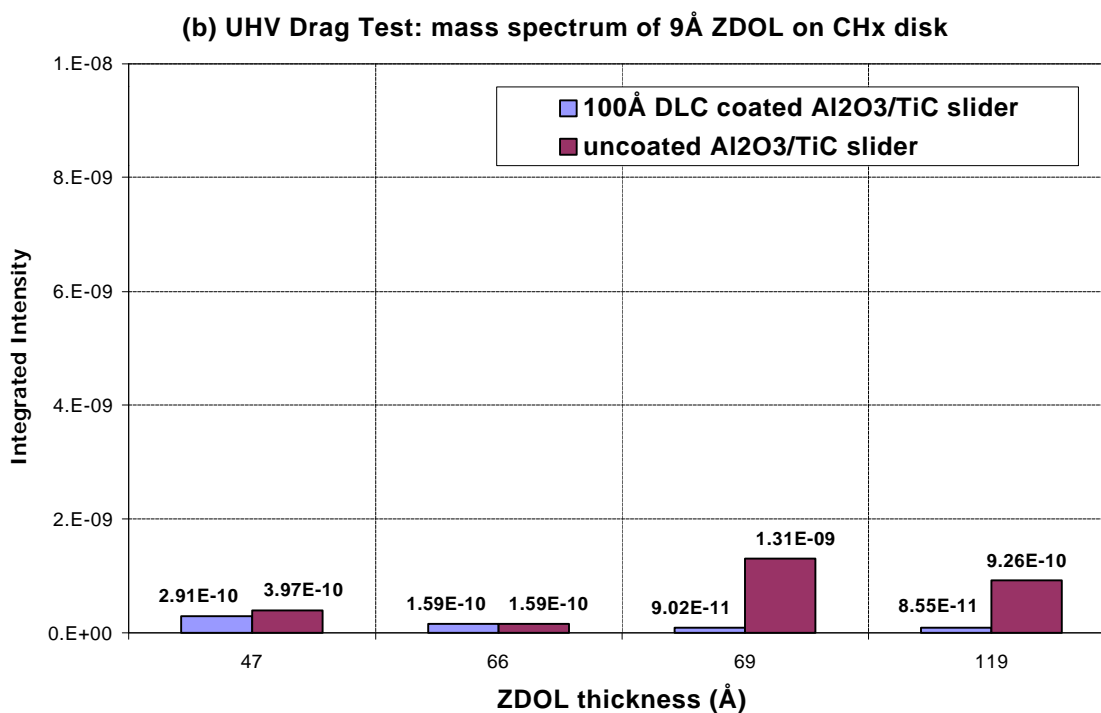
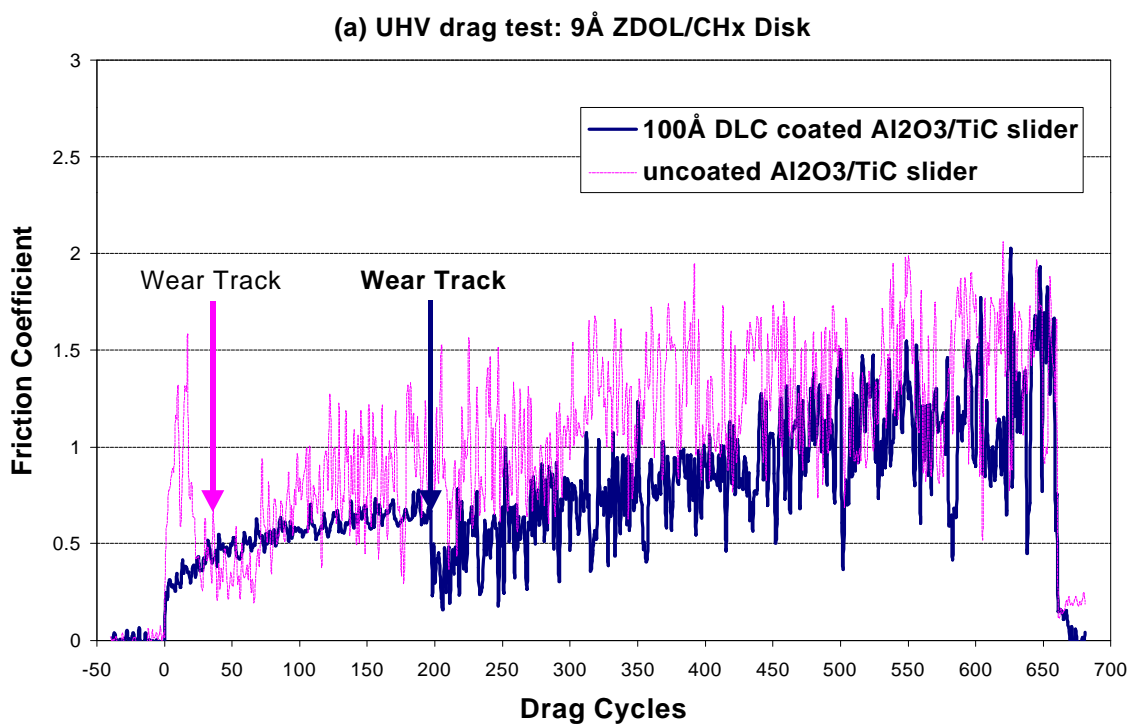
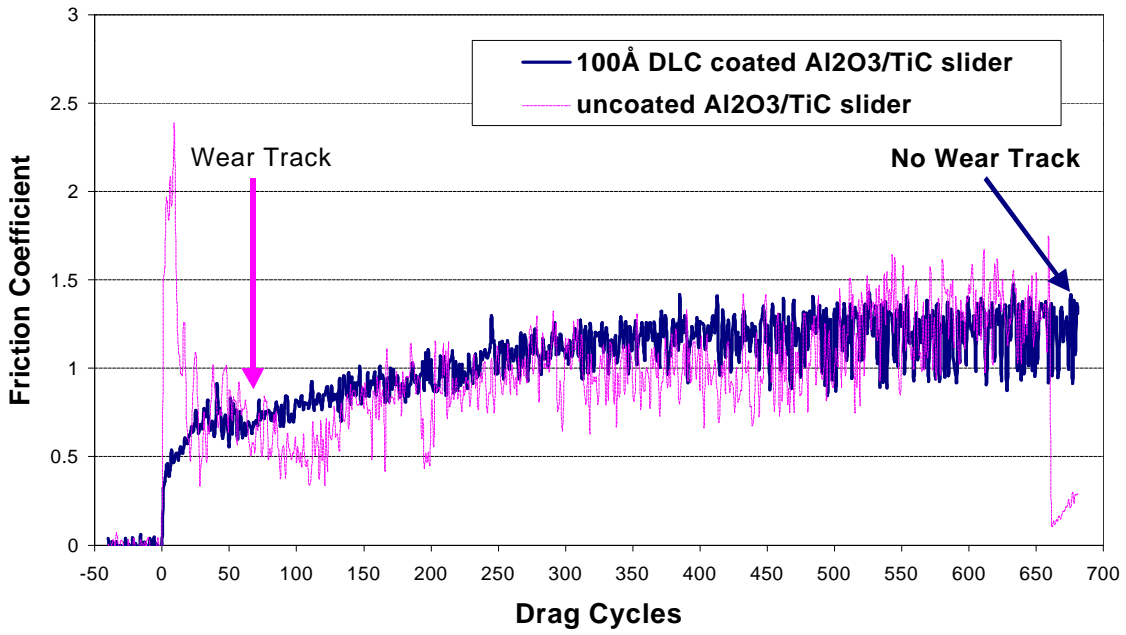


Figure 3: (a) friction coefficient of UHV drag test on 9 Å ZDOL lubricated disk; (b) mass spectrum of four major ZDOL decomposition fragments.

(a) UHV drag test: 12.5Å ZDOL/CHx Disk



(b) UHV Drag Test: mass spectrum of 12.5Å ZDOL on CHx disk

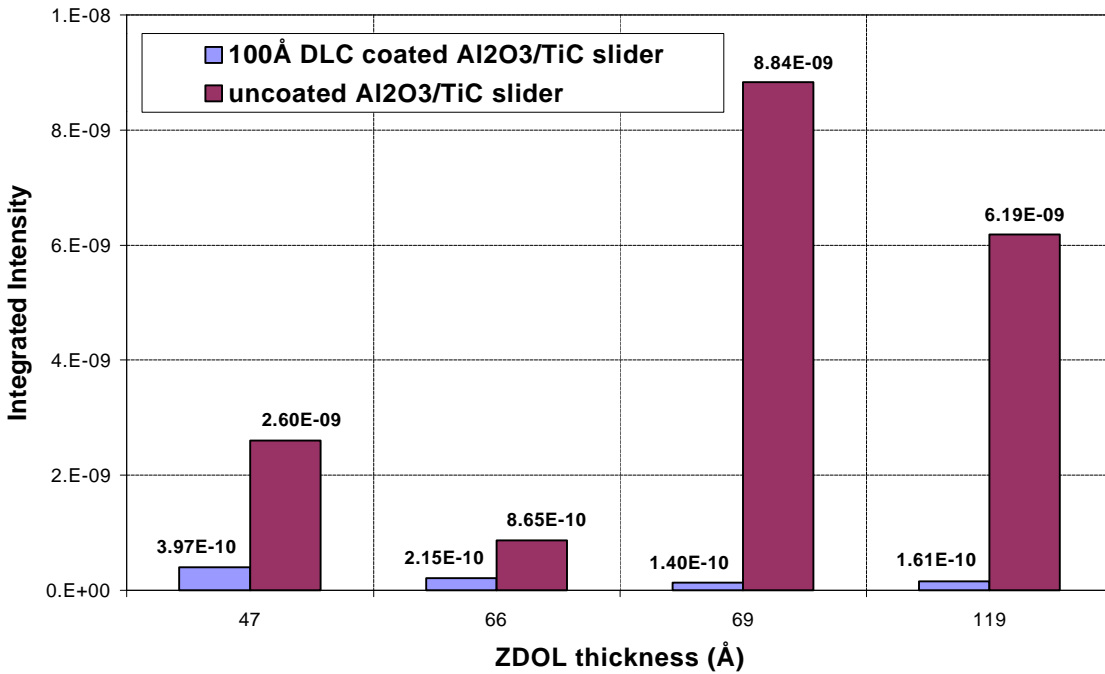
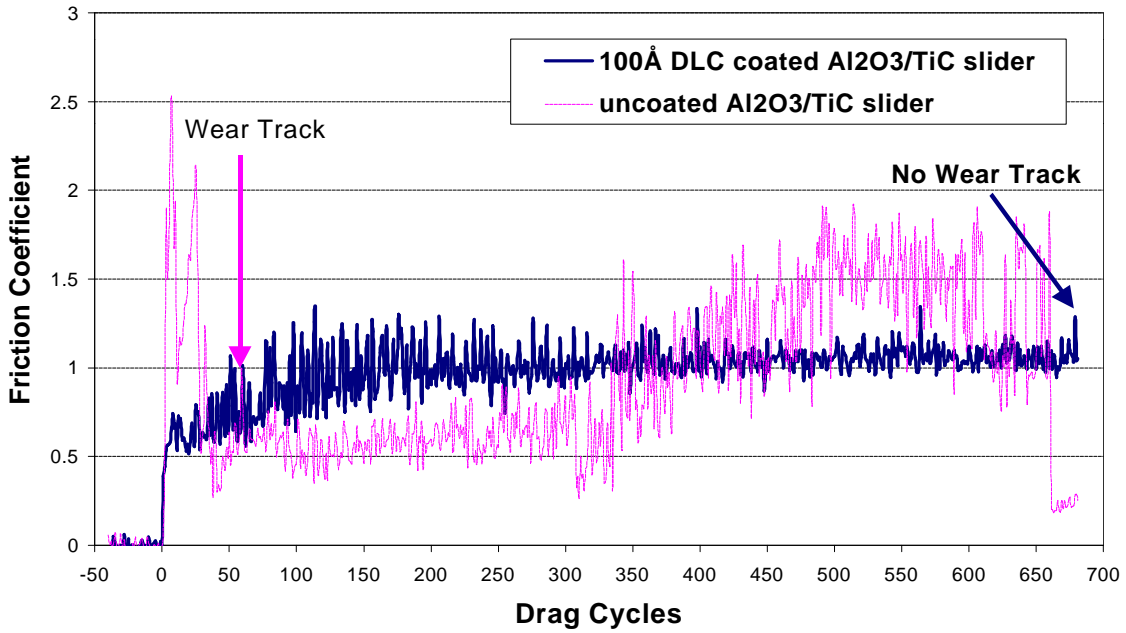


Figure 4: (a) friction coefficient of UHV drag test on 12.5Å ZDOL lubricated disk; (b) mass spectrum of four major ZDOL decomposition fragments.

(a) UHV drag test on 15.4Å ZDOL/CHx Disk



(b) UHV Drag Test: mass spectrum of 15.4Å ZDOL on CHx disk

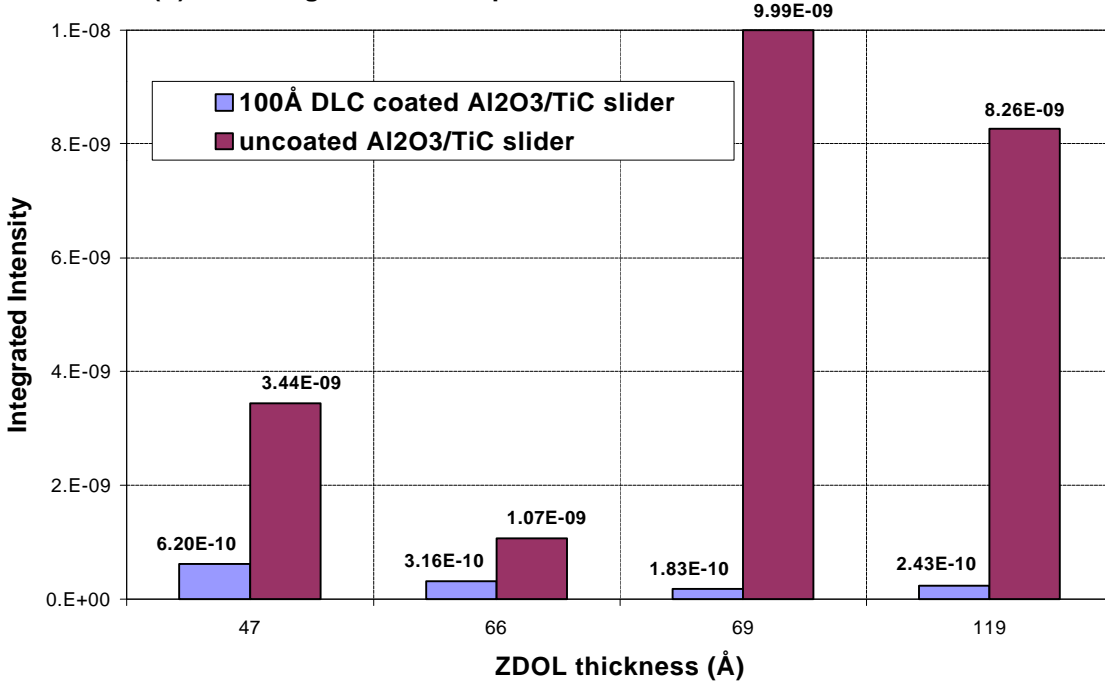
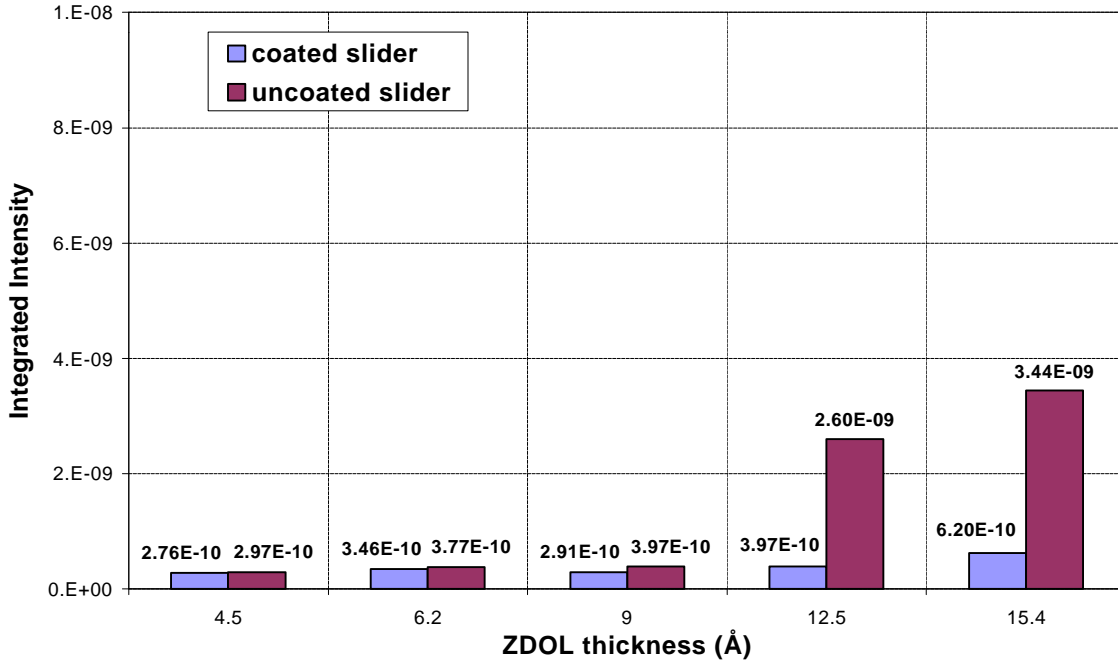


Figure 5: (a) friction coefficient of UHV drag test on 15.4Å ZDOL lubricated disk; (b) mass spectrum of four major ZDOL decomposition fragments.

(a) UHV Drag Test: Degradation Intensity of Mass 47 (CFO)



(b) UHV Drag Test: Degradation Intensity of Mass 66 (CF₂O)

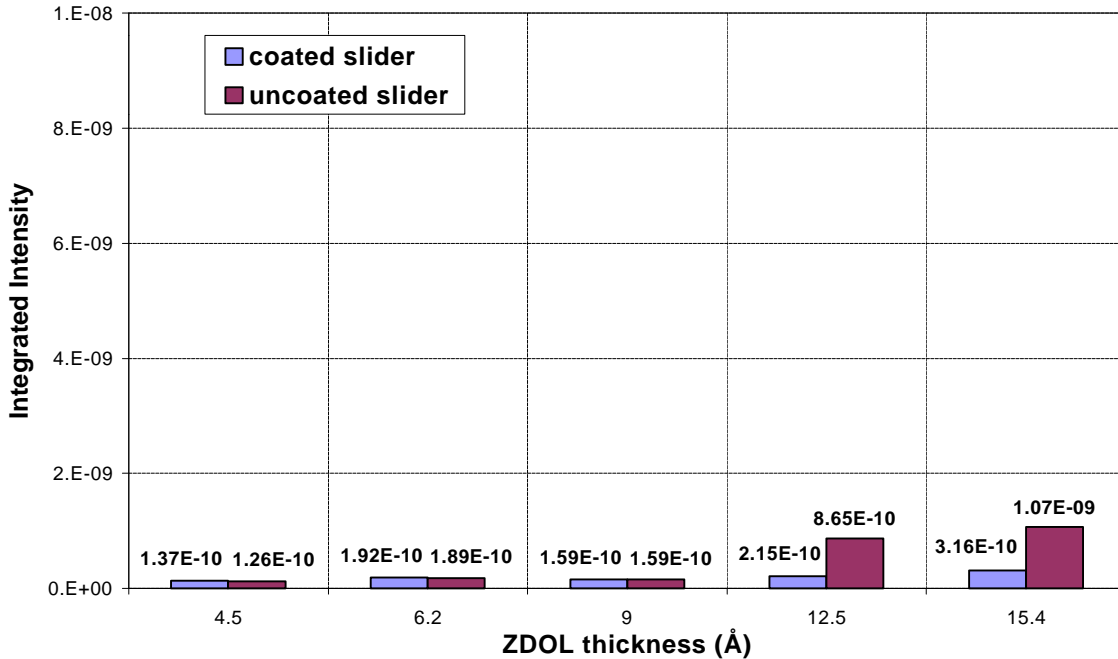


Figure 6: integrated degradation intensity of ZDOL during UHV drag tests on CH_x disks with different ZDOL thickness. Two major decomposition fragments occur under frictional action: (a) mass 47 (CFO), and (b) mass 66 (CF₂O).

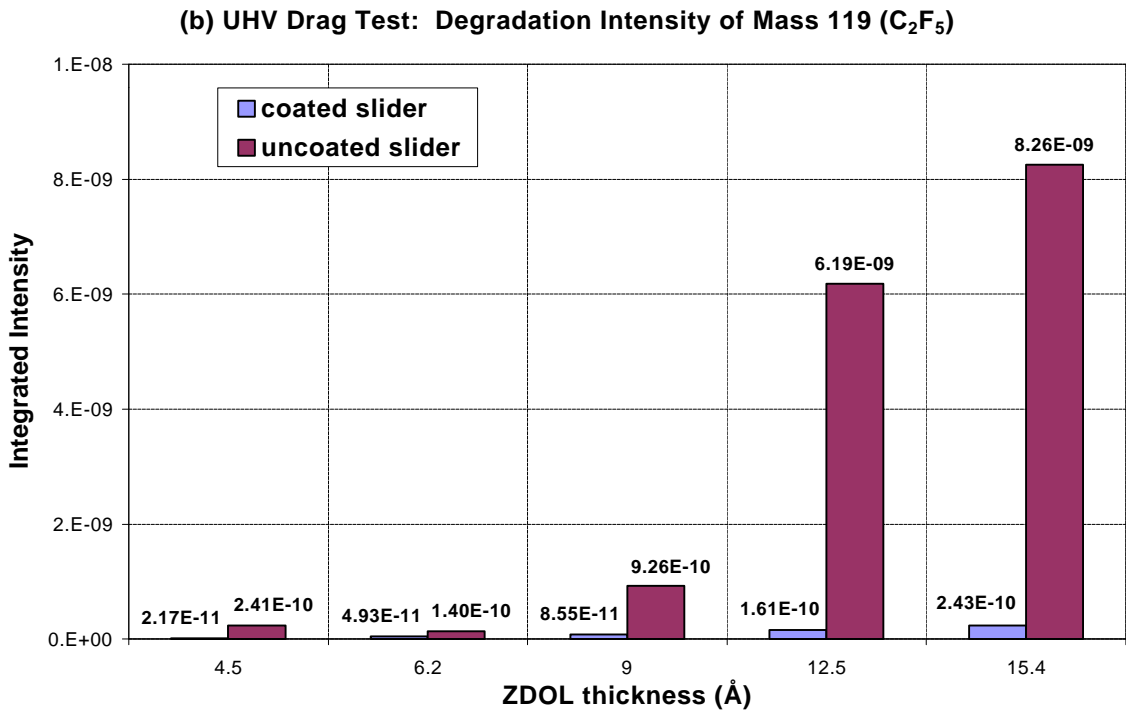
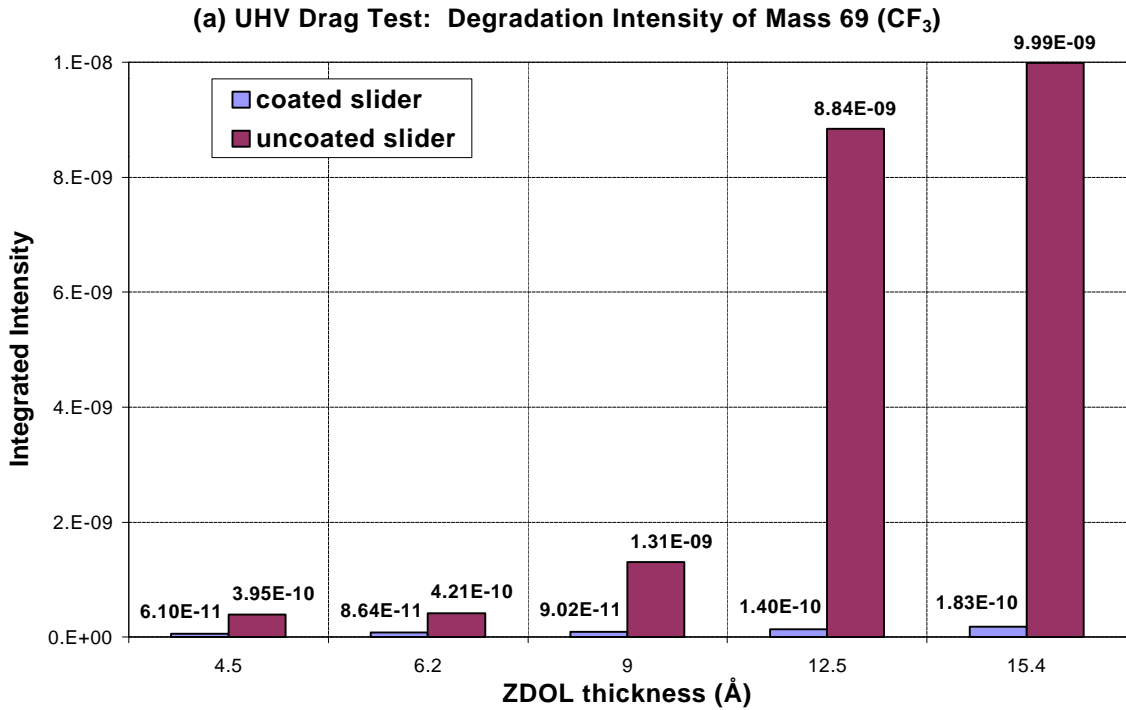


Figure 7: integrated degradation intensity of ZDOL during UHV drag tests on CH_x disks with different ZDOL thickness. Two major decomposition fragments occur under catalytic reaction: (a) mass 69 (CF₃), and (b) mass 119 (C₂F₅).

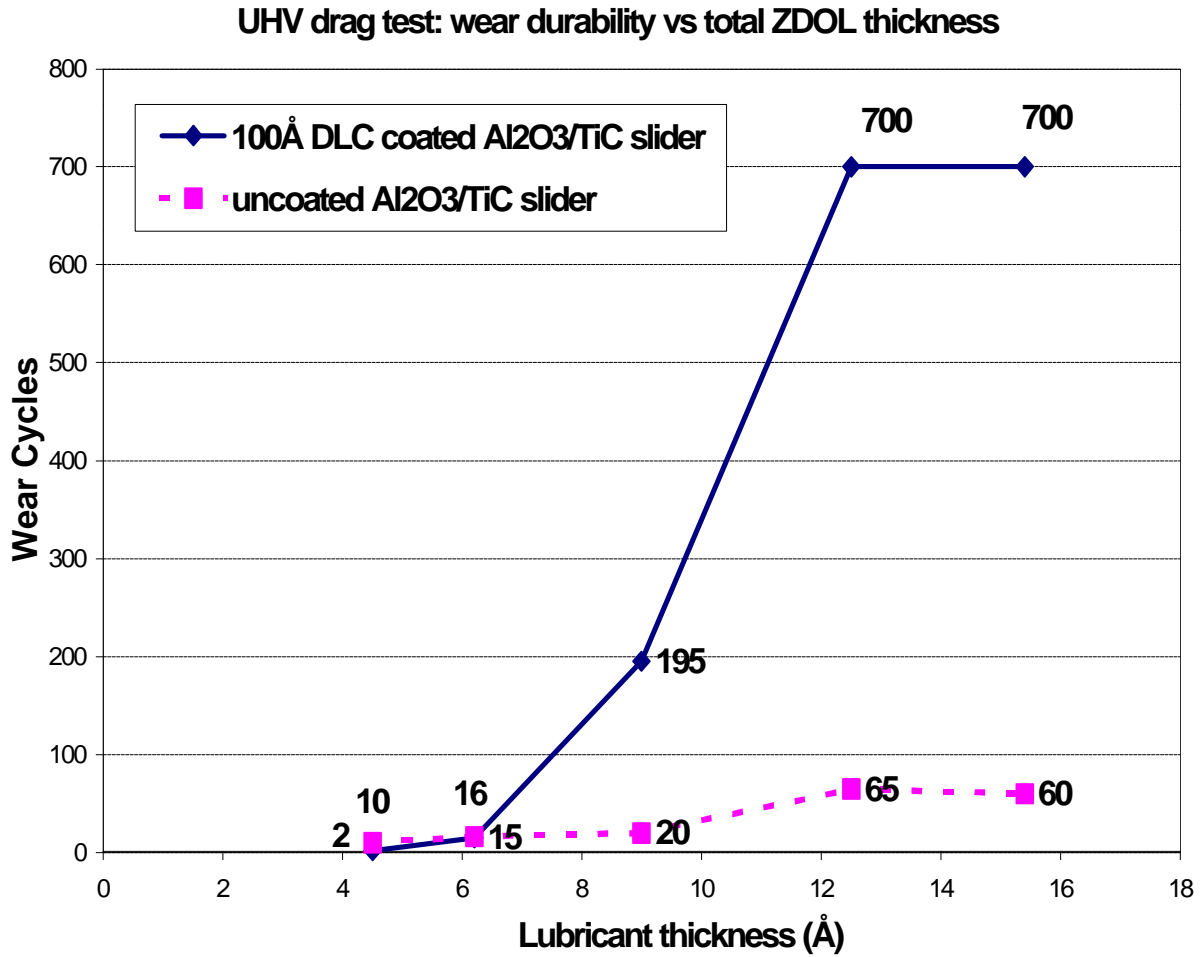


Figure 8: wear durability of CHx disks with different ZDOL thickness during UHV drag tests with DLC coated or uncoated Al₂O₃/TiC sliders.

UHV Drag Test: wear durability vs mobile ZDOL thickness

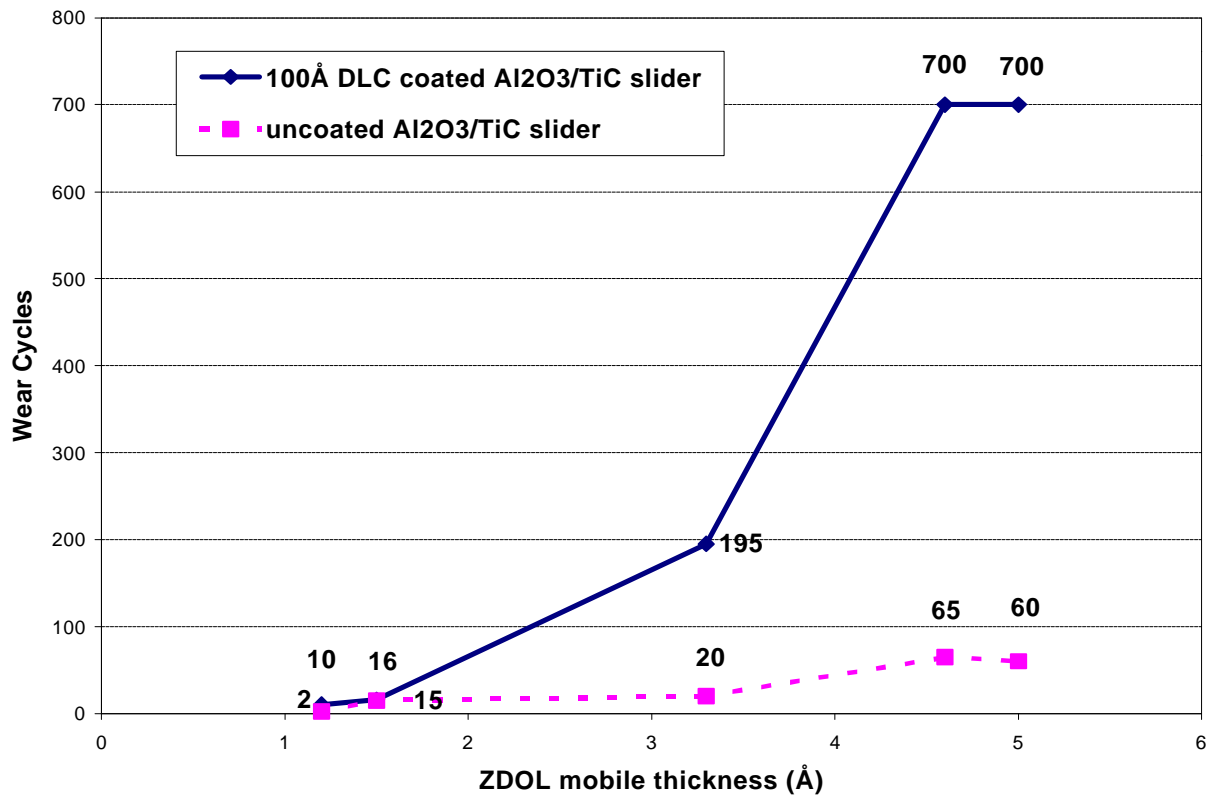


Figure 9: wear durability of CHx disks with different mobile ZDOL thickness during UHV drag tests against DLC coated or uncoated Al₂O₃/TiC sliders.

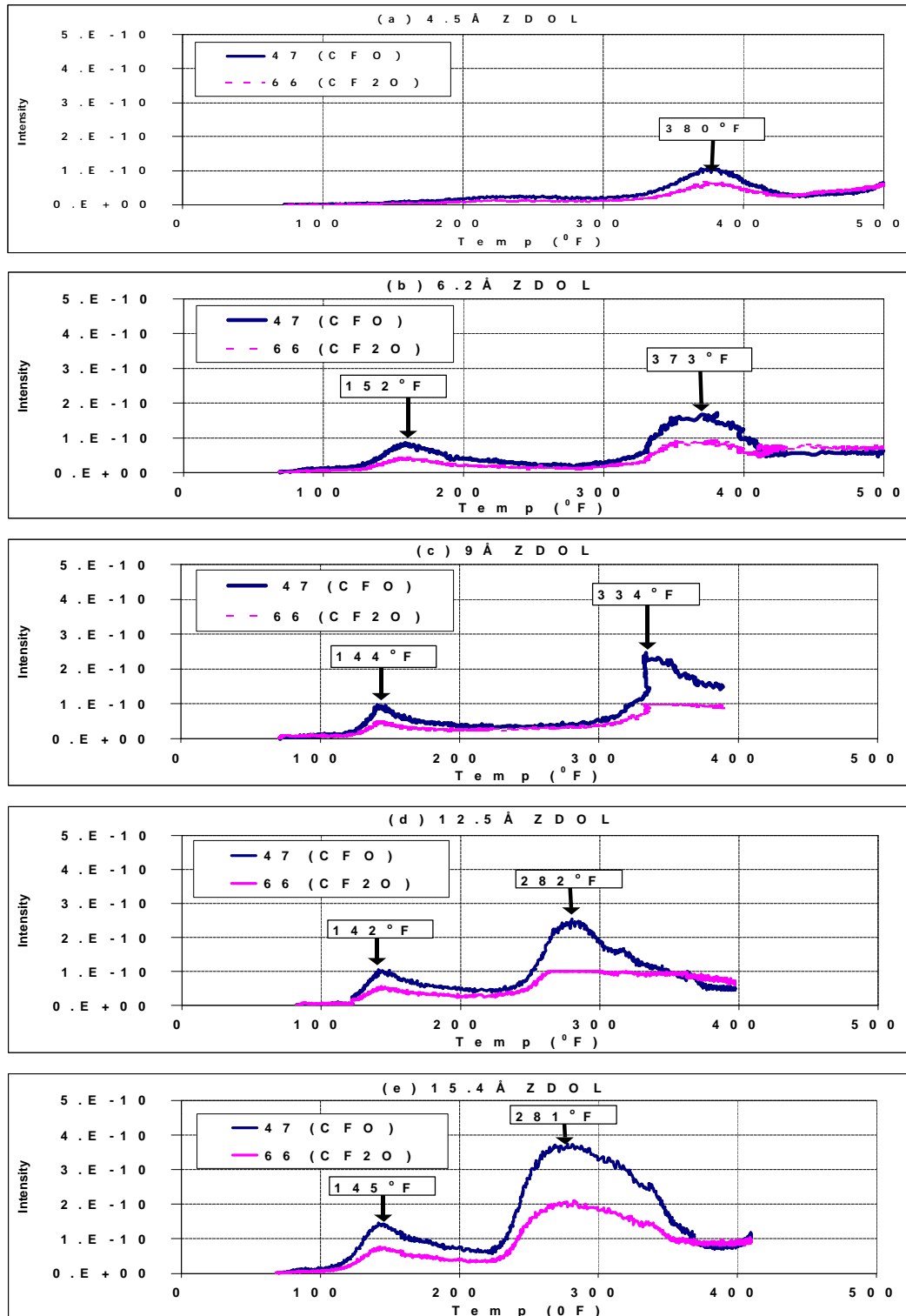


Figure 10: history profiles of mass 47 (CFO), and mass 66 (CF₂O) during the thermal desorption tests of CHx disks with ZDOL thickness ranging from 4.5Å to 15.4Å.

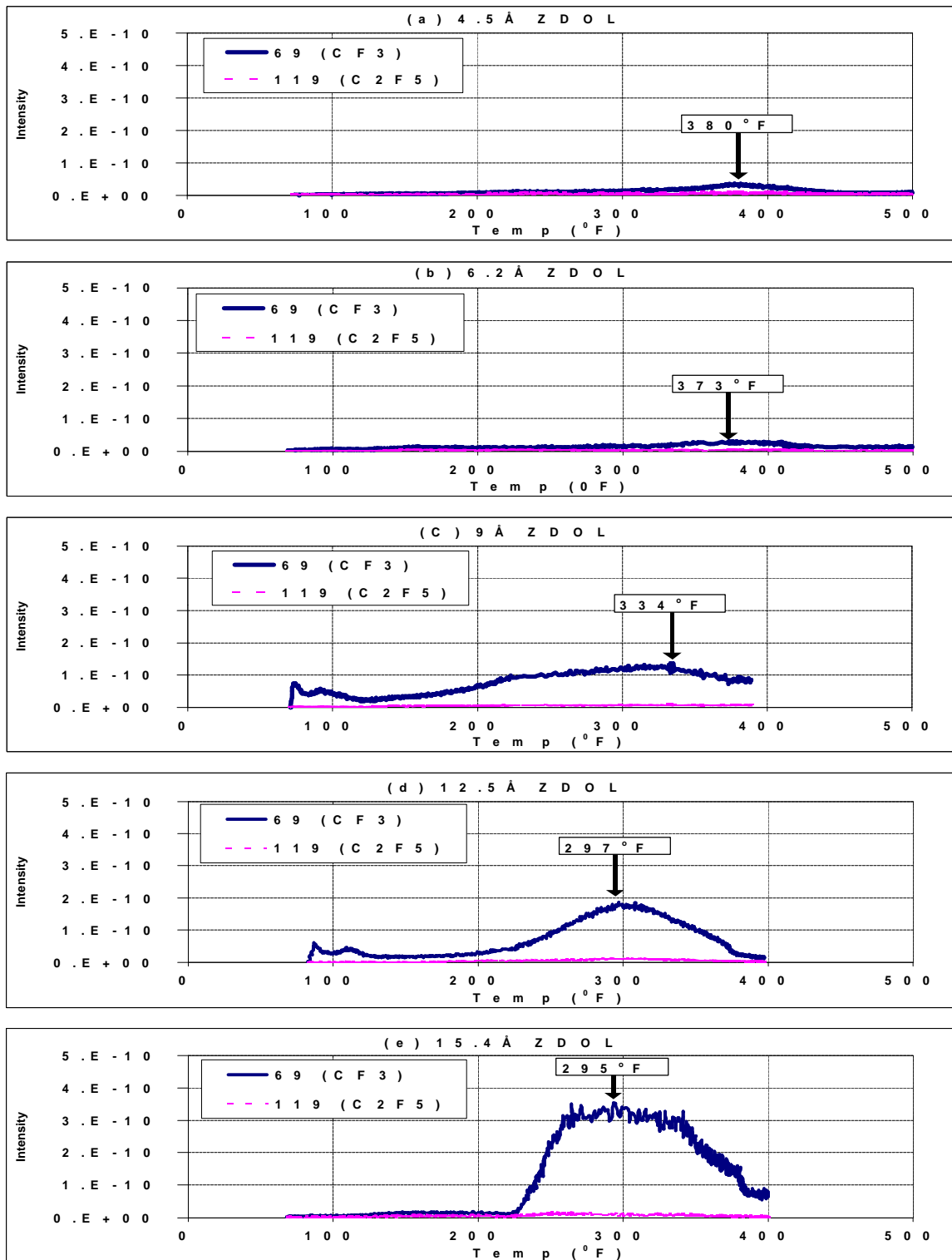


Figure 11: history profiles of mass 69 (CF₃), and mass 119 (C₂F₅) during the thermal desorption tests of CHx disks with ZDOL thickness ranging from 4.5Å to 15.4Å.

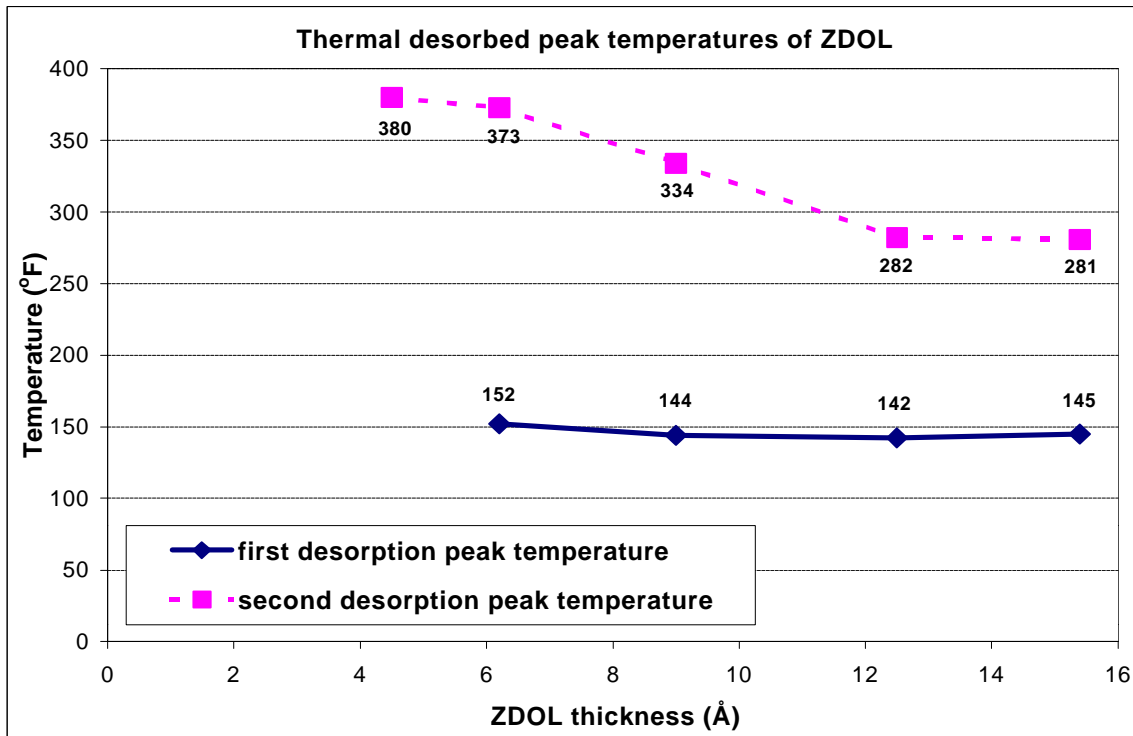


Figure 12: thermal desorption peak temperatures of ZDOL for CHx disks with ZDOL thickness ranging from 4.5Å to 15.4Å.

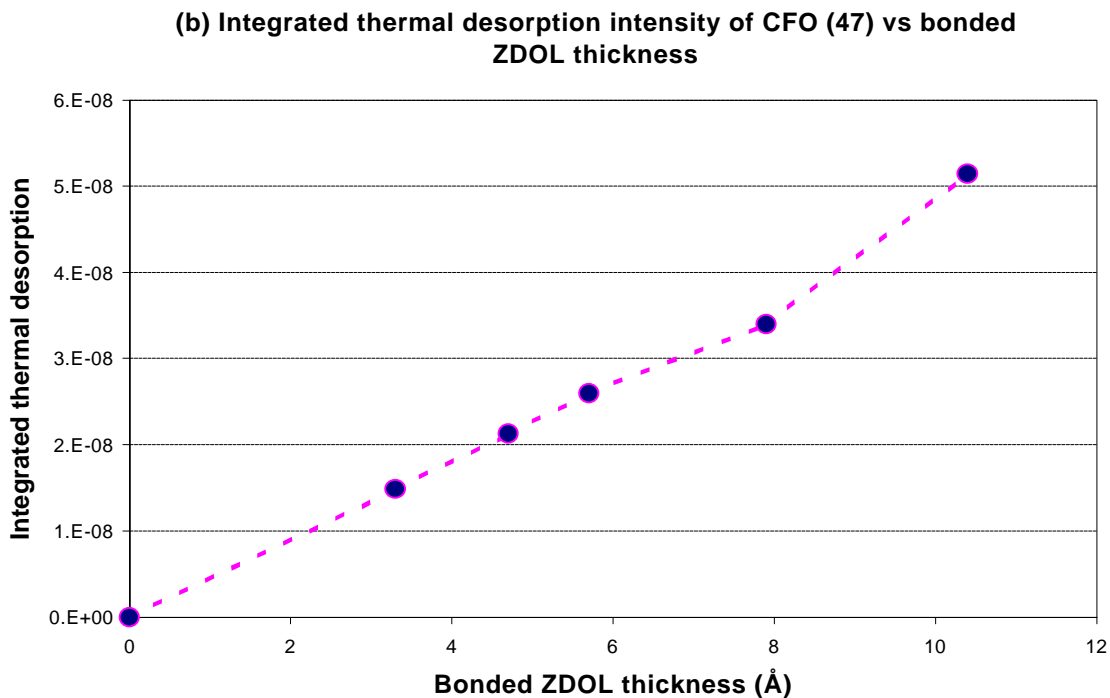
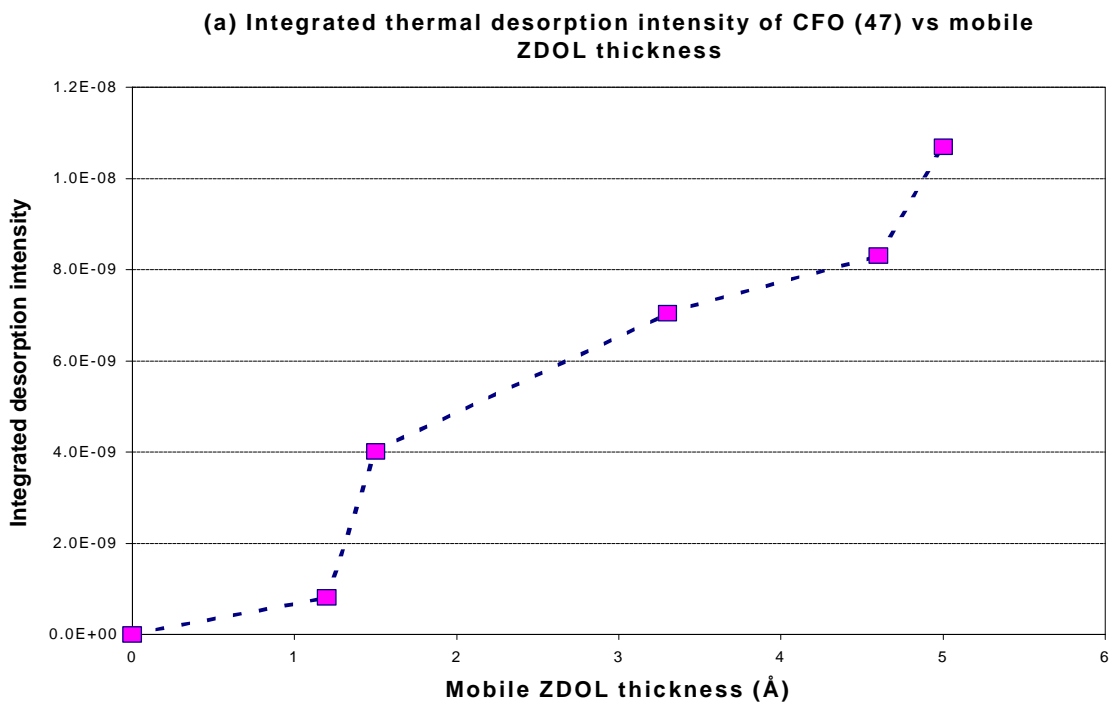


Figure 13: integrated thermal desorption intensity of CFO (47) versus (a) **mobile** ZDOL thickness during the first desorption peak, and (b) **bonded** ZDOL thickness during the second desorption peak.